RSC Advances

ROYAL SOCIETY OF CHEMISTRY

www.rsc.org/advances

Controllable dye adsorption behavior on amorphous tungsten oxide nanosheet surfaces

Jian Yi Luo,* Yu Rong Lin, Bao Wen Liang, Yu Dong Li, Xi Wei Mo, and Qing Guang Zeng

School of Applied Physics and Materials, Wuyi University, Jiangmen, Guangdong, 529020, P. R. China

* Authors to whom correspondence should be addressed, E-mail: luojiany@mail3.sysu.edu.cn (J. Y. Luo)

Abstract:

In this paper, the surface interactions between the different dyes and amorphous WO_3 nanosheets in water were investigated. The amorphous WO_3 nanosheets had a strong adsorption for cationic dyes, and could be self-precipitated from water after they absorbed enough dye molecules in their micro-structures. The absorbed cationic dyes eventually formed *H*-aggregates or *J*-aggregates on the surfaces of WO_3. Conversely, the amorphous WO_3 nanosheets had a weak or no any adsorption capacity for anionic dyes. This selective adsorption property of WO_3 nanosheets could be applied to separate cationic dyes from mixed solution. The possibilities of pH-induced desorption for cationic dyes on the WO_3 nanosheet surfaces had also been demonstrated in this paper, and its mechanism had been discussed in depth. The findings leaded to a better outstanding of the dye adsorption behavior on the amorphous tungsten oxide surfaces.

Keywords: dye adsorption; amorphous WO_3 nanosheets; selective adsorption; pH-induced desorption

* Authors to whom correspondence should be addressed, E-mail: luojiany@mail3.sysu.edu.cn (J. Y. Luo)

1. Introduction

Adsorption of organic dyes on the surfaces of materials became a research topic earliest due to the aim of the removal of dyes from wastewater, and the typical adsorbent materials included rice husk, clay, powdered activated sludge, and activated carbon.[1-5] Recently, aggregations of dye molecules have been intensively investigated due to their applications on the forward-looking technologies, such as the solid-state dye lasers, light energy conversions systems, chemical sensors, high-resolution optical imaging, drug delivery and photodynamic therapy.[6, 7] There has been considerable research interest focused on the study of organic dye monolayer adsorbed chemically on metal oxide semiconductors, especially organic dye on TiO_2 for enhancing visible-light absorption in the dye-sensitized solar cells. [8-11]

Tungsten oxide had been intensively investigated as one of interesting photoelectron materials, due to its potential applications on electrochromic and photochromic devices, gas sensors devices, and field emission devices.[12-16] More recently, the surface interactions between organic dyes and tungsten oxide nanomateirals has also attracted more and more attentions. The photochromic WO_3 nanocolloid particles had exhibited colorimetric sensing properties for α-amino acid compounds in aqueous solution, which can be applied in continuous in vivo monitoring.[17] The novel dyes adsorption property of amorphous WO_3 nanostructures has been concerned by Xiao *et al.*[18] and our group.[19] Recently, the pH-responsive switchable aggregation phenomena of xanthenes dyes adsorbed on tungsten oxide colloid surface has been reported by K. Adachi and his coworkers.[20] However, the abovementioned research works were focused on dye adsorption behaviors on metal oxide surfaces, but less attention is paid to its controlled switching between dye adsorption and desorption, which is a crucial technology for the controlled-dyes adsorption on the surfaces of metal oxide semiconductors.

In this paper, we focus our interest on the controllable dye adsorption behavior

on the amorphous tungsten oxide (a-WO_3) nanosheet surfaces. Our results here clearly revealed that the a-WO_3 nanosheets only had a strong adsorption for cationic dyes in water, and this selective adsorption property could be applied to separate the cationic dyes from mixed solution. The possibility of pH-induced desorption for cationic dyes on the a-WO_3 nanosheet surfaces had also been demonstrated in this paper

2. Experimental Section

Material Synthesis and Characterization: The amorphous WO_3 nanosheets were synthesized on the normal glass substrate by thermal evaporation deposition, described as below: The pure WO_3 powder (99.95%) was put in a tungsten boat, and was heated at the condition of high vacuum (4.0×10^{-3} Pa) by increasing the electric current of the tungsten boat to 130 A, and keeping it at 130 A for 30 minutes. The WO_3 vapor would deposit on the glass substrate (which had been placed above the tungsten boat) to form the a-WO_3 nanosheets. The temperature of the substrate was kept at 250℃ during the deposition process by another heater. The as-grown WO_3 nanosheets could be separated from the substrate into the deionized water by ultrasonic cleaning for one hour in water, and then were dried into adsorbent powder. The morphologies, chemical compositions, and crystal structures of the prepared products were characterized by field emission scanning electron microscopy (SEM, Nova Nano SEM 432), X-ray diffraction spectroscopy (XRD, X'pert Pro with Cu Kα radiation), and high-resolution transmission electron microscopy (TEM, FEI Tecnai GZ F30 at 300 kV), respectively. The size distribution and Zeta potential tests of WO_3 nanosheets in the solution were analyzed by a laser particle analyzer (Malvern Zetasizer Nano ZS90)**.**

Dyes Adsorption Test: Seven typical kinds of dye molecules in industrial wastewater were used to test the adsorption property of a-WO_3 nanosheets. These dyes included methylene blue (MB), rhodamine B(RhB), magenta red (MR), methyle violet (MV), methyl orange (MO), chrome black T(CBT) and acide chrome blue (ACB), in which the former four ones belonged to cationic dyes and the other three

ones belonged to anionic dyes. The test experiment for the a-WO_3 nanosheets powders could be described as follows: The *N* mg adsorbent was adding into 100 ml deionized water, and was suspended 10 min by an ultrasonic concussion. The suspended solution was divided into ten copies of 10 ml test solutions with the same adsorbent of *N*/10 mg. Then, 20 ml dye solution with the initial concentration of C_o was added and stirred into 10 ml test solution, and the dye concentration C_T in test solution became to $2C_o/3$. As a comparison, a blank solution which was a mixed solution of 10 ml deionized water without adsorbent and 20 ml dye solution with the initial concentration of C_o should be prepared simultaneously. In the statement below, it often was expressed as that *N*/10 mg adsorbent powder was added into a dye solution (30 ml, $2C_o/3$) for simplicity. Here, it should be noted that we assumed the suspended solution was totally uniform, but in the actual case, some large-sized suspended WO_3 nanosheets maybe precipitated at the bottom of the solution, inducing the difference of the amount of WO_3 nanosheets in the different solutions. In order to test the uniformity of the suspended solution, a laser particle analyzer (Malvern Zetasizer Nano ZS90) was applied to probe the dynamic light scattering (DLS) spectra from different detecting positions (See the supplementary material). The DLS result as shown in Fig. S1 showed that the particle size distribution spectra from the upper to bottom sections of the suspended solution were almost totally overlapped, indicating the suspended solution was uniform. Thus, the abovementioned assumption is reasonable.

Additionally, in order to test the dye adsorption property as-grown thin WO_3 film on the substrate, the WO_3 film with an area of 1.5 cm × 2 cm was injected into the dye solution, and was allowed to stand for 4 hours in solution. The changes in the absorption spectra of the test solutions during the dye adsorption onto the a-WO_3 nanosheets were recorded by using a UV-Vis spectrophotometer (Shimadzu UV2550).

Dyes Separation Experiment: A cationic dye solution (e.g., MB solution) was added into an anionic dye solution (e.g., MO solution) to form a mixed dye solution. Then, the a-WO_3 nanosheets powder was used to adsorb the cationic dye molecules in the mixed solution. The change of the mixed dye solutions during the adsorption was

recorded by the absorption spectrophotometer.

pH-induced dye desorption Experiment: 3.4 mg a-WO_3 nanosheets powder was added into a MO solution (20 mg/L, 30 ml), and then after the adsorption finished (e.g., the absorption spectra of the test solutions did not change over time), H_2O_2 (25 %) or $NH_3 \cdot H_2O$ (30%) was added drop by drop to decrease or increase the pH value of the solution under magnetic stirring. The corresponding change in absorption spectrum was also recorded the absorption spectrophotometer.

3. Results and Discussion

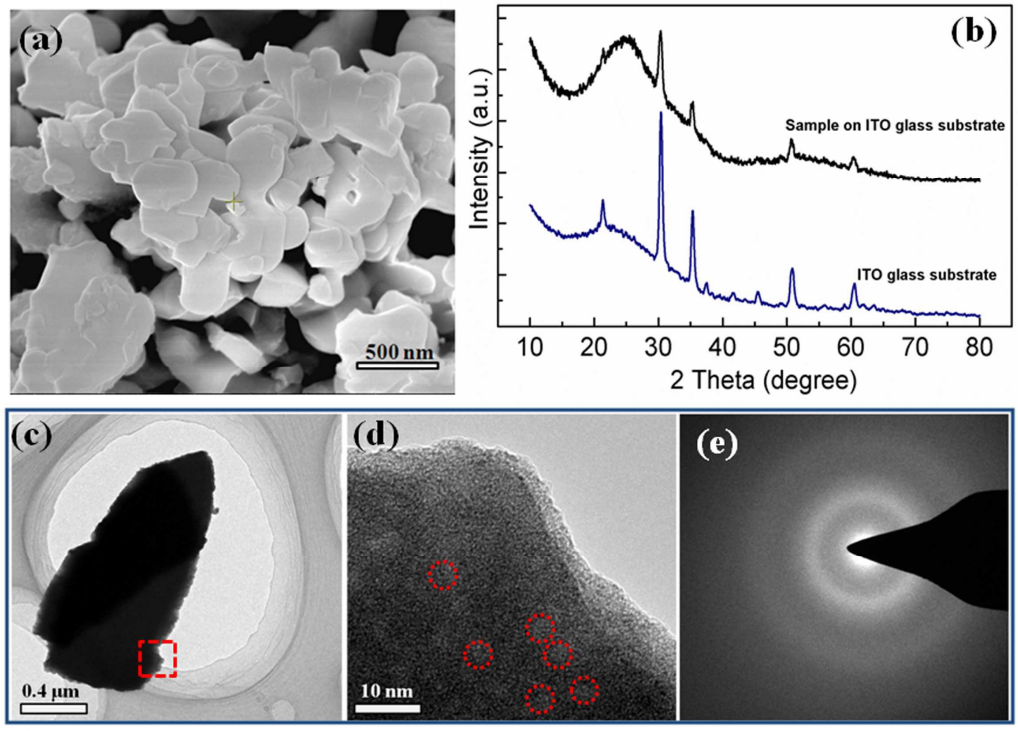

Fig. 1 (a) SEM image of the WO_3 nanosheets separated from the substrate. (b)XRD spectra of the WO_3 nanosheets on ITO glass substrate (the one for ITO glass substrate has also been given). (c) Typical low-resolution TEM image Of a WO_3 nanosheet. (d) Enlarge TEM image and (e) SAED pattern of the red-dashed-square region in (c).The positions of pore microstructures are denoted by small red-dashed circles in (d).

As shown in **Fig. 1(a)**, the produces had a sheet-sharp structure, which could be more easily recognized in the SEM image of the as-prepared produces on the substrate as shown in Fig. S2 (See the supplementary material). The sizes of nanosheets were in the range of 200-2000 nm, and their crystalline structures of the nanosheets were analyzed by XRD test. The XRD results as shown in **Fig. 1(b)** showed that only a broad peak centered at 24 degrees came from the sample, and all sharp diffraction came from the ITO glass substrate. This broad peak at 24 degrees could be indexed to the superposition of three strongest characterized peaks (002), (020), and (200) of monoclinic WO_3 (JCPDs cards: 43-1035). This indicated the amorphous characteristic of the nanosheets. This amorphous characteristic had also been proved by TEM test results as shown in **Fig.1(c-e)**. As shown in **Fig. 1(d)**, some small white regions which were denoted by small red-dashed circles were observed in the internal structure of the nanosheet. Since the contrast in TEM image represents the intensity of transmission electrons, the white region indicates the transmission electron intensity is stronger than the other regions, and it means the thick of this region should be thinner than the other regions. Thus, in our TEM test, the white spots in the enlarged TEM image could be attributed to the appearance of the pore microstructures in WO_3 nanosheets. Additionally, no periodic structure could be seen from the high-resolution TEM image. Selected-area electron diffraction (SAED) pattern as shown in **Fig. 1(e)** showed there were only amorphous diffraction rings without any crystal diffraction spots, further confirming the amorphous characteristic of produces.

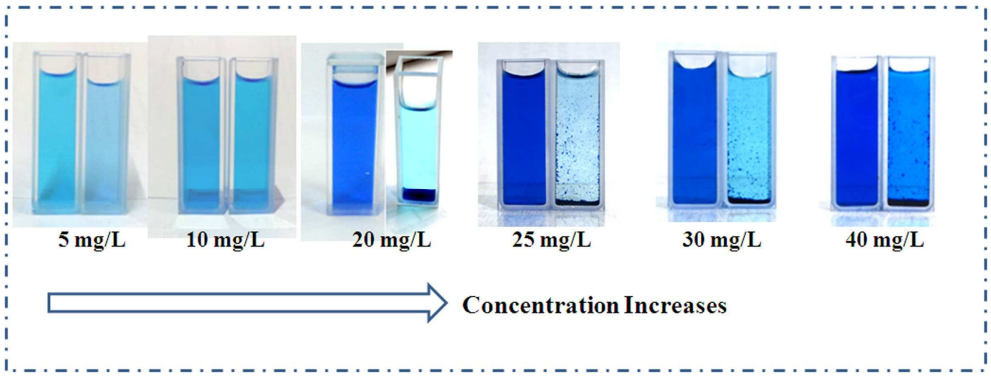

Fig. 2. Self-precipitation phenomenon when WO_3 nanosheets are absorbed by enough MB molecules: Photographs at left and right side are the MB solutions before and after the introduction of the WO_3 nanosheets with the same mass of 1.4 mg into the solutions in each concentration, respectively.

The dye adsorption property of the a-WO_3 nanosheets was investigated by the removal typical dyes molecules from water. As a typical result shown in **Fig. 2**, the WO_3 nanosheets had a high adsorption property for MB dyes from aqueous solution, and the saturated MB adsorbed amount can reach to 600 mg/g, which had been reported in our previous work.[19] Furthermore, a self-precipitation phenomenon of the adsorbent would occur when the MB concentration in water increased to be higher that a certain threshold (e.g., 20 mg/L in **Fig. 2**. This value could change with the mass of adsorbent used, and its corresponding threshold adsorbed amount was at about 420 mg/g), in the case of the same solution volume and the mass of the adsorbent used. This had been proved to be attributed to the density increase of a-WO_3 nanosheets after their porous micro-structures were adsorbed with enough MB molecules.[19] This may be useful for the separation of the nanoscale adsorbents from water. Additionally, the as-grown nanosheets on the substrate without separated into water also had high performance on cationic dyes adsorption. As shown in **Fig. 3**, a WO_3 film with an area of 1.5 cm × 2.0 cm on the glass substrate was injected into RhB dye solution (8 mg/L, 20 ml), and was allowed to stand for one hour in solution. As the result shown in the photograph of **Fig. 3(b)**, the color of solution turned transparent and the RhB molecules original in the water totally adsorbed onto the surface of WO_3 nanosheets film. The change of RhB solution was simultaneously recorded by the absorption spectrum as shown in **Fig. 3(c)**. The strongest absorption peak centered at 550 nm which was attributed to light absorption of RhB molecules almost disappeared after the adsorption by the WO_3 thin film, indicating that most of RhB molecules in water had been removed out by the thin film.

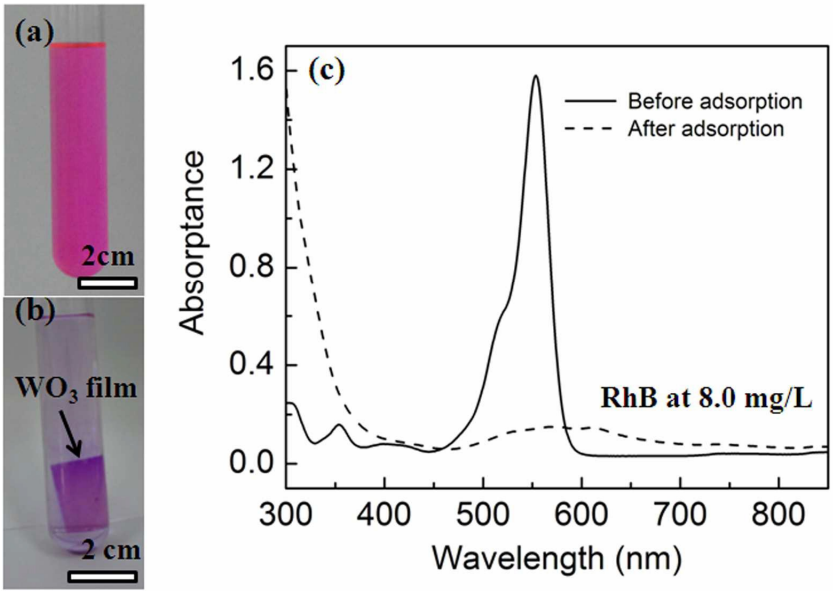

Fig. 3. (a), (b) Photographs of the RhB solutions with a concentration at 8.0 mg/L before and after the introduction of a piece of amorphous WO_3 film into the solutions. (c) The corresponding absorption spectra of the RhB solutions before and after adsorption by amorphous WO_3 film.

Another feature in cationic dye adsorption of the a-WO_3 nanosheets was its Aggregation phenomena of cationic dyes on the adsorbent surfaces. The typical results were shown in **Figs. 4(a, b)**, in which a blue-shift absorption and a red-shift absorption compared to the monomer band could be assigned to the formation of two kinds of aggregate geometries, namely *H*- and *J*-aggregates on the WO_3 surfaces, respectively.[21] In the MB adsorption, only H-aggregates occurred, while both of *H*- and *J*-aggregates could happen in the case of RhB adsorption. This result for RhB adsorption agreed with the recent report work from K. Adachi and his coworkers.[20] However, this Aggregation adsorption could not happen for the anionic dyes. As shown in **Figs. 4(c, d)**, the characteristic peaks for MO and CBT dyes in absorption spectra were almost unchanged after the adsorption compared to the ones before adsorption. Only change was the enhance absorption intensity at the ultraviolet region, which could be attributed to the band-edge absorption of WO_3 nanosheets in water,

since WO_3 is a wide gap n-type semiconductor with band gap at 2.6-3.0 eV , agreed with our previous work.[22]

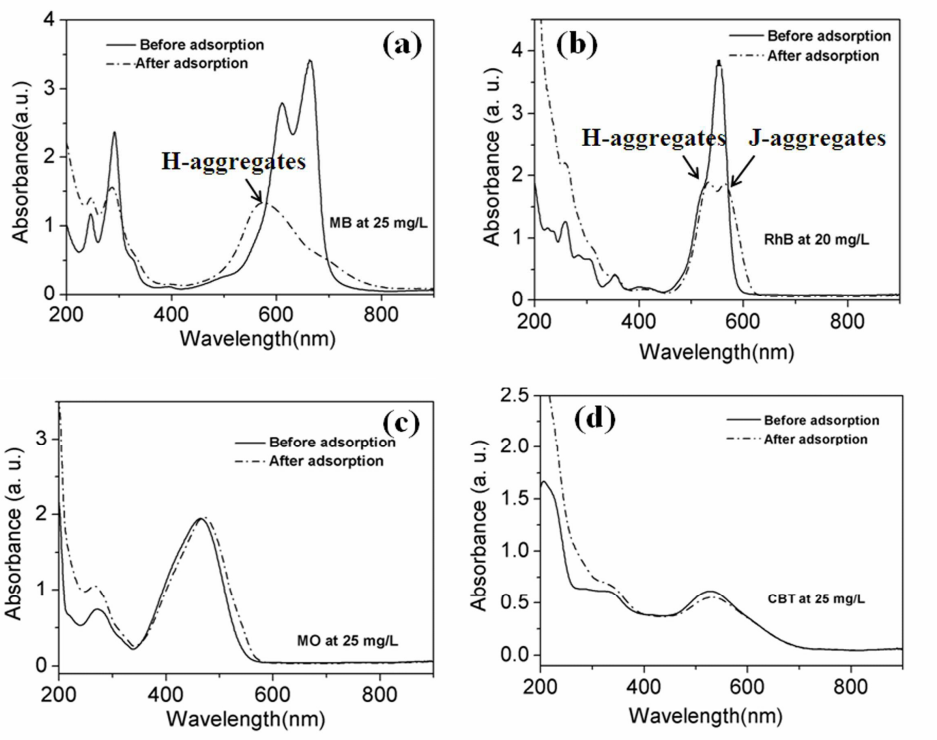

Fig. 4. Absorption spectra for four typical dyes solutions before and after adsorption by the amorphous WO_3 nanosheets with the same mass of 3.5 mg in the dye solutions(30 ml): (a) MB solution at 25 mg/L, (b) RhB solution at 20 mg/L, (c) MO solution at 25 mg/L, (d) CBT solution at 20 mg/L.

Seven typical kinds of dyes adsorptions had been tested for our nanosheets. These dyes included methylene blue (MB), rhodamine B(RhB), magenta red (MR), methyle violet (MV), methyl orange (MO), chrome black T(CBT) and acide chrome blue (ACB), in which the former four ones belonged to cationic dyes and the other three ones belonged to anionic dyes. The test results as shown in **Fig. 5** clearly indicated that WO_3 nanosheets only had a strong adsorption for cationic dyes, and had a weak or no any adsorption for anionic dyes. The adsorbed amount Q_e (mg/g), i. e.,

the amount of dye adsorbed into unit weight of the adsorbent, which is usually used to evaluate the dye adsorption ability of an adsorbent, can be expressed by

$$Q_e = \gamma C_o V / m \quad (1a)$$

$$\gamma = (1 - C_e / C_o) \times 100\% \quad (1b)$$

Here, γ is defined as decolor rate. C_o and C_e are the dye concentration before and after adsorption, respectively. V is the volume of dye solution used (L), and m is the mass of adsorbent used (g) (here, m equals 0.0035g). The decolor rate and adsorbed amount for the abovementioned seven kinds of dyes had been listed in Tab. 1. For all cationic dyes, the adsorbed amount exceeded 70 mg/g, while it was lower than 12 mg/g for anionic dyes. This selective adsorption property of the nanosheets was remarkable.

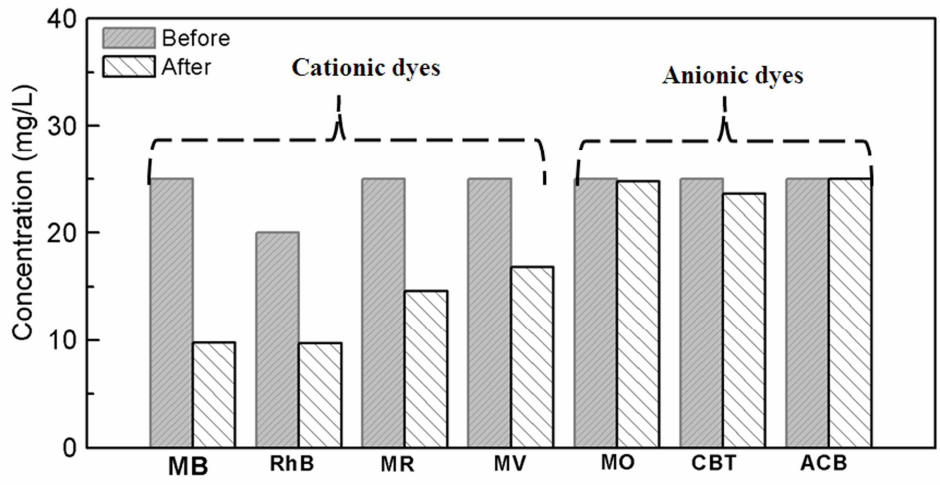

Fig. 5. The changes in the concentration of seven kinds of test dyes solution before and after the adsorption by the 3.5 mg amorphous WO_3 nanosheets in 30 ml solution (MB: methylene blue, RhB: rhodamine B, MR: magenta red, MV: methyle violet , MO: methyl orange, CBT: chrome black T, ACB: acide chrome blue).

Tab. 1. List of decolor rate and adsorbed amount of WO_3 nanosheets for different kinds of dyes

Dyes	C_0V (mg)	γ (%)	Q_e (mg/g)
MB	0.75	61	130.7
RhB	0.60	51.5	88.3
MR	0.75	41.7	89.4
MV	0.75	32.8	70.3
MO	0.75	1.0	2.1
CBT	0.75	5.5	11.8
ACB	0.75	0	0

This selective adsorption property implied that the surface charges of WO_3 nanosheets may be negative, and the selective adsorptions resulted from the electrostatic attractive/repulsive interactions between the WO_3 nanosheets and dyes molecules. In order to distinguish the kind of surface charges of WO_3 nanosheets, a Zeta potential test for WO_3 nanosheets was carried out in deionized water. The test result as shown in **Fig. 6** clearly indicated the Zeta potential of WO_3 nanosheets was negative, and the average value was in the range from -21 to -15 mV, proving our abovementioned analysis about the surface charges of WO_3 nanosheets.

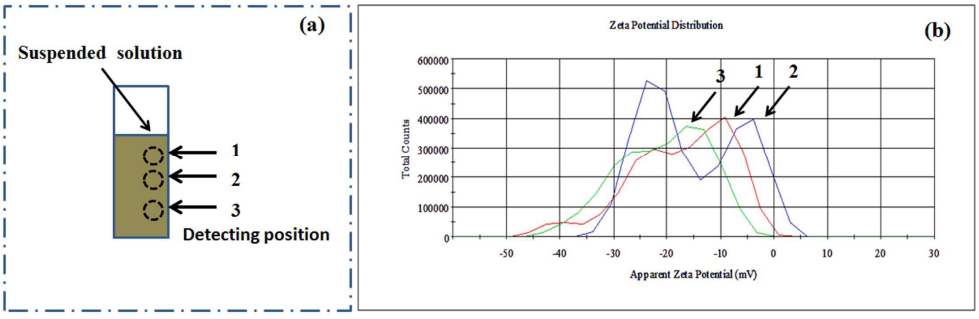

Fig. 6. (a) Schematic diagram illustrating the detecting position of Zeta potential tests for WO_3 nanosheets in the deionized water: upper, middle and bottom sections of the

suspended solution are numbered as 1, 2, and 3, respectively; (b) The corresponding Zeta potential curves and their average Zeta potentials are (1) -17.3, (2)-15.4, and (3) -20.7 mV, respectively.

The selective adsorption property of WO_3 nanosheets can be applied to separate the cationic dyes from mixed solution. As an example, 10 ml MB dye solution (an cationic dye solution,15 mg/L) was added into 10 ml MO solution (an anionic dye solution, 15 mg/L) to form a mixed dye solution, and 3.5 mg WO_3 nanosheets powder was used to adsorb the cationic dye molecules in the mixed solution. The results were shown in **Fig. 7**. Before adsorption, the mixed solution was deep green, and after the introduction of WO_3 nanosheets into the solution, the mixed solution gradually turned yellow from deep green. This change process was also recorded by an absorption spectrophotometer, and the corresponding absorption spectra of the solutions were show in **Figs. 7(a-d)**. Both characteristic absorption peaks from methylene blue (MB) molecules and methyl orange (MO) molecules could be observed in the absorption spectrum of the mixed solution before adsorption, but after adsorption the ones from MB molecules disappeared and only the ones from MO molecules could be observed. It means that the MB molecules were almost totally removed from water by the adsorption of WO_3 nanosheets, and MO molecules were left in water, achieving the separation cationic dyes from the solution. Here, it should be pointed out that the absorbance intensity of mixed solution in **Fig. 7(g)** decreased to half of the ones in MB solution in **Fig. 7(e)** or MO solution in **Fig. 7(f)** before mixing, which was due to the increase of solvent (water here) volume to 30 ml from 15 ml, resulting the concentrations of MB and MO molecules in solution to drop down.

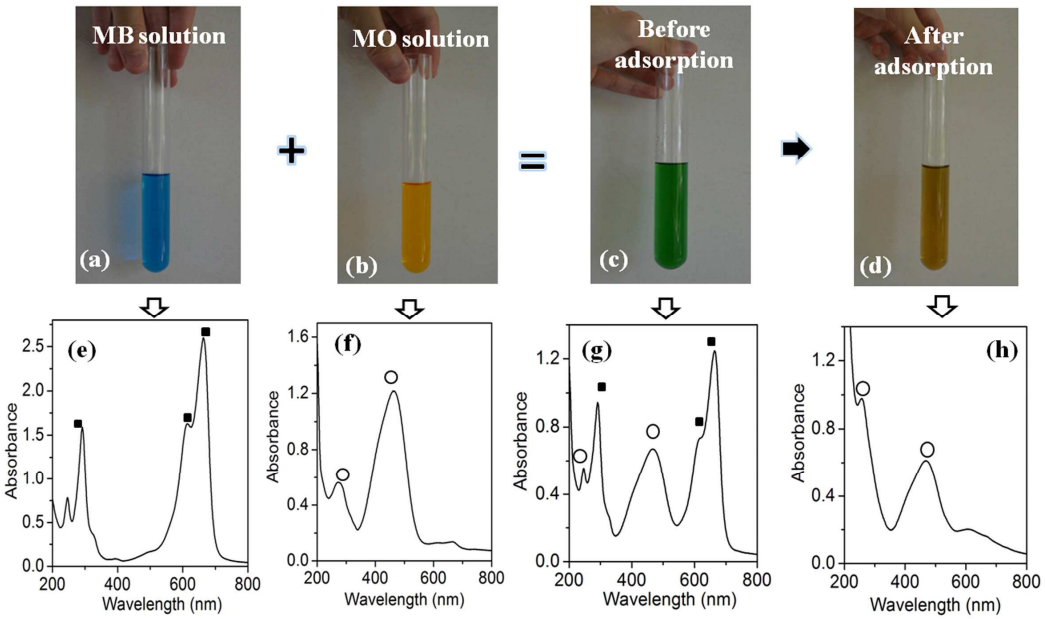

Fig. 7. Dye-separation experiment: Photographs of (a) 10 ml MB solution with the concentration of 15 mg/L, (b) 10 ml MO solution with the concentration of 15 mg/L, and their mixed solution (c) before and (d) after adsorption by 3.5 mg amorphous WO_3 nanosheets in solution. (e-h) are the corresponding absorption spectra of the solutions in (a-d). Small black squares and white circles indicate the characteristic absorption peaks from MB molecules and MO molecules in water, respectively.

The question rises as to how to separate the adsorbed cationic dyes from the a-WO_3 nanosheets. In order to study the dye desorption processes on the surfaces of amorphous WO_3 nanosheets, we altered the pH values of the solutions by the introduction of a little hydrogen peroxide or ammonia water into the test solutions. Hydrogen peroxide and ammonia water would get through the following reaction equations (Eqs. (2a-3b)) to create hydrogen ions (H^+) and hydroxyl ions (OH^-) in the solution, respectively.

$$H_2O_2 \leftrightarrow H^+ + HO_2^- \quad (2a)$$

$$HO_2^- \leftrightarrow H^+ + O_2^- \quad (2b)$$

$$NH_3 + H_2O \leftrightarrow NH_3 \bullet H_2O \quad (3a)$$

$$NH_3 \bullet H_2O \leftrightarrow NH_4^+ + OH^- \quad (3b)$$

The result as shown in **Fig. 8(a)** clearly indicated that the MB desorption processes from the surfaces of WO_3 nanosheets strongly depended on the pH value of the solution. In the neutral (pH 7.7, the value of the pure MB solution) solution, two absorption peaks centered at 665 and 610 nm which could be assigned to the MB monomers and dimers in water had shifted to the peak at 560 nm after adsorption, and this blue-shift effect was barely influenced by the pH value decreased from 7.7 to 2.0). This peak at 560 nm had been proved to be attributed to the aggregate formation, namely *H*-dimers of MB molecules on the surfaces of the a-WO_3 nanosheets according to the previous reports.[23-26] Thus, most MB molecules in water had adsorbed onto the surfaces of the WO_3 nanosheets in the neutral solution, and they were hard to be desorbed from the WO_3 nanosheets by an acidic treatment. On the other hand, when the pH value increased to more than 8.0, the new appearing peak at 560 nm after adsorption shifted back to 665 and 610 nm, indicating the adsorbed MB molecules could be desorbed from WO_3 nanosheets into water by an alkaline treatment. Thus, we had demonstrated the dye adsorption and desorption on the surfaces of WO_3 nanomaterials could be controlled by pH value. However, it should be noted that the WO_3 nanosheets with cleaned surfaces after desorption were still suspended in the solution. Thus, another question rises as to how to recycle these nanomaterials in solution. We still had not good idea to solution this question so far. Thus, the reusability of the WO_3 nanomaterials should be considered as a crucial question in our further work.

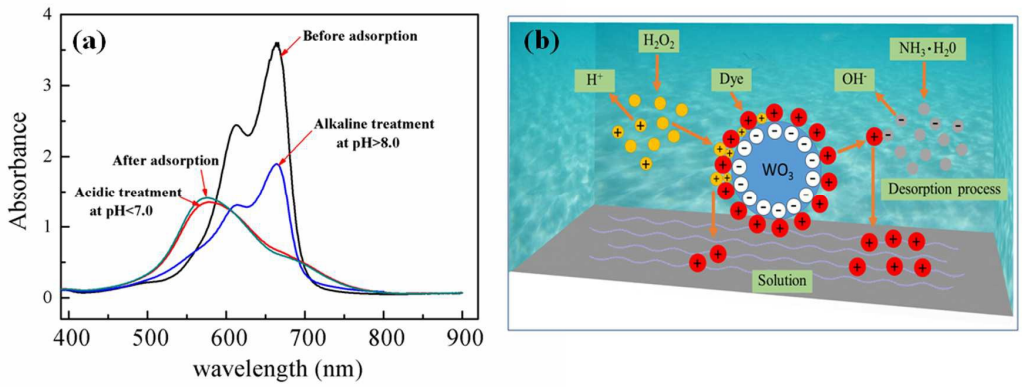

Fig. 8. (a) pH-induced desorption of MB molecules on the surfaces of WO_3 nanosheets. (b) Schematic diagram illustrating cationic dyes desorption processes in the acidic and alkaline treatments, respectively.

At last, the dyes desorption processes involve the acidic and alkaline treatments were proposed to be as the illustration in **Fig. 8(b)**. Firstly, in the neutral solution, the cationic dyes adsorbed onto the negatively surface-charged WO_3 nanosheets due to the electrostatic attraction. Then, when H_2O_2 was introduced into the solution, some new produced hydrogen ions (H^+) may occupy some surface positions of WO_3 nanosheets, resulting in a slight decline in the adsorption amount, but most new produced hydrogen ions could not reach the surfaces of WO_3 nanosheets due to the repulsive forces from the adsorbed dye molecules. Thus, the acidic treatment could not induce the adsorbed cationic dyes to get away from WO_3 nanosheets. Conversely, in an alkaline treatment, once hydroxyl ions (OH^-) were introduced into the solution, they would be attracted with the adsorbed dye molecules on the surfaces of WO_3 nanosheets, and the charged dye molecules would be neutralized, leading the dyes to escape from the negatively surface-charged WO_3 nanosheets.

4. Conclusions

In summary, the amorphous WO_3 nanosheets were fabricated by a one-step thermal evaporation without any catalyst, and their dye adsorption properties were studied in depth. The dye adsorption test showed that the WO_3 nanosheets had a

strong adsorption for cationic dyes in water, and they could be self-precipitated from water after they absorbed enough dye molecules in their porous micro-structures. The evidences in experiments in this study proved that cationic dyes was adsorbed onto surfaces of WO_3 nanosheets by an electrostatic attractive interaction between the negative charging surfaces of WO_3 nanosheets and cationic dyes molecules, and these adsorbed dyes molecules had an aggregation phenomenon on the surfaces of WO_3 nanosheets. Seven kinds of dye adsorption had been tested and the results clearly indicated that the WO_3 nanosheets had a selective adsorption property for cationic dyes, and this property could be applied to separate the cationic dyes from the dyes mixed solution. Thus, the findings in this work not only prove the outstanding dye adsorption capacity of the amorphous WO_3 nanomaterials in water, but also demonstrated their potential application on dyes separation technologies.

Acknowledgments

The authors gratefully acknowledge the financial support of the projects from the National Natural Science Foundation of China (No. 51402218), Guangdong Natural Science foundation (Nos. 2014A030313622, and 2015A030306031), and Science Foundation for Young Teachers of Wuyi University (Nos. 2013zk05, and 2014td01).

Notes and references

[1] J. J. Li, J. T. Feng, and W. Yan, *Appl. Surf. Sci.*, 2013, **279**, 400-408.

[2] E. Forgacs, T. Cserháti, and G. Oros, *Environ. Int.*, 2004, **30**, 953-971.

[3] T. G. Chuah, A. Jumasiah, I. Azni, S. Katayon, and S. Y. Thomas Choong, *Desalination*, 2005, **175**, 305-316.

[4] G. Crini, *Bioresource Technology*, 2006, **97**, 1061-1085.

[5] R. Malik, D. S. Ramteke, and S. R. Wate, *Waste Management*, 2007, **27**, 1129-1138.

[6] B. L. Feringa, and W. R. Browne, *Molecular Switches*, Wiley-VCH, Germany, 2011.

[7] J. L. Atwood, and J. W. Steed, *Encyclopedia of Supramolecular Chemistry*, Marcel Dekker, New York, USA, 2004.

[8] K. G. Reddy, T. G. Deepak, G. S. Anjusree, S. Thomas, S. Vadukumpully, K. R. V. Subramanian, S. V. Nair, and A. S. Nair, *Phys. Chem. Chem. Phys.*, 2004, **16**, 6838-6858.

[9] J. Gong, J. Liang, and K. Sumathy, *Renewable and Sustainable Energy Reviews*, 2012, **16**, 5848-5860.

[10] H. Kim, and J. S. Suh, *RSC Adv.*, 2015, **5**, 74107-74114.

[11] D. Qi, L. Wang, and J. Zhang, *RSC Adv.*, 2015, **5**, 74557-74561.

[12] C. G. Granqvist, *Sol. Energy Mat. Sol. Cells*, 2000, **60**, 201-262.

[13] J. Y. Luo, X. X. Chen, W. D. Li, W. Y. Deng, W. Li, H. Y. Wu, L. F. Zhu, and Q. G. Zeng, *Appl. Phys. Lett.*, 2013, **102**, 113104.

[14] H. Zheng, J. Z. Ou, M.S. Strano, R. B. Kaner, A. Mitchell, and K. Kalantar-zadeh, *Adv. Funct. Mater.*, 2011, **21**, 2175-2196.

[15] J. W. Liu, J. Zheng, J. L. Wang, J. Xu, H. H. Li, and S. H. Yu, *Nano Lett*., 2013, **13**, 3589-3593.

[16] C. X. Zhao, S. Z. Deng, N. S. Xu, and J. Chen, *RSC Adv.*, 2015, **5**, 70059-70063.

[17] S. Tanaka, K. Adachi, and S. Yamazaki, *Analyst*, 2013, **138**, 2536-2539.

[18] W. Xiao, W. T. Liu, X. H. Mao, H. Zhu, and D. H. Wang, *J. Mater. Chem. A*, 2013, **1**, 1261-1269.

[19] J. Y. Luo, Z. Cao, F. Chen, L. Li, Y. R. Lin, B. W. Liang, Q. G. Zeng, M. Zhang, X. He, and C. Li, *Appl. Surf. Sci.*, 2013, **287**, 270-275.

[20] K. Adachi, K. Watanabe, and S. Yamazaki, *Ind. Eng. Chem. Res*., 2014, **53**, 13046-13057.

[21] M. Kasha, H. R. Rawls, amd M. A. El-Bayoumi, *Pure Appl. Chem.*, 1965, **11**, 371-392.

[22] J. Y. Luo, S. Z. Deng, Y. T. Tao, F. L. Zhao, L. F. Zhu, L. Gong, J. Chen, and N. S. Xu, *J. Phys. Chem. C*, 2009, **113**, 15877-15881.

[23] W. Spencer and J. R. Sutter, *J. Phys. Chem.*, 1979, **83**, 573-1576.

[24] K. Bergmann and C. T. Ọkonski, *J. Phys. Chem.*, 1963, **67**, 2169-2177.

[25] S. M. Ohline, S. Lee, S. Williams, and C. Change, *Chem. Phys. Lett.*, 2001, **346**, 9-15.

[26] A. A. Attia, W. E. Rashwan, and S. A. Khedr, *Dyes and Pigments*, 2006, **69**, 128-136.